

Machine Learning-Derived Echocardiographic Phenotypes Predict Heart Failure Incidence in Asymptomatic Individuals

Masatake Kobayashi, Olivier Huttin, Martin Magnusson, João Pedro Ferreira, Erwan Bozec, Anne-Cecile Huby, Gregoire Preud'Homme, Kevin Duarte, Zohra Lamiral, Kevin Dalleau, et al.

▶ **To cite this version:**

Masatake Kobayashi, Olivier Huttin, Martin Magnusson, João Pedro Ferreira, Erwan Bozec, et al.. Machine Learning-Derived Echocardiographic Phenotypes Predict Heart Failure Incidence in Asymptomatic Individuals. JACC: Cardiovascular Imaging, 2021, S1936-878X (21), pp.00556-8. 10.1016/j.jcmg.2021.07.004 . hal-03357064

HAL Id: hal-03357064
https://hal.univ-lorraine.fr/hal-03357064

Submitted on 28 Sep 2021

HAL is a multi-disciplinary open access archive for the deposit and dissemination of scientific research documents, whether they are published or not. The documents may come from teaching and research institutions in France or abroad, or from public or private research centers.

L'archive ouverte pluridisciplinaire **HAL**, est destinée au dépôt et à la diffusion de documents scientifiques de niveau recherche, publiés ou non, émanant des établissements d'enseignement et de recherche français ou étrangers, des laboratoires publics ou privés.



Distributed under a Creative Commons Attribution - NonCommercial - NoDerivatives 4.0 International License

JACC: CARDIOVASCULAR IMAGING VOL. ■, NO. ■, 2021
© 2021 THE AUTHORS. PUBLISHED BY ELSEVIER ON BEHALF OF THE AMERICAN COLLEGE OF CARDIOLOGY FOUNDATION. THIS IS AN OPEN ACCESS ARTICLE UNDER THE CC BY-NC-ND LICENSE (http://creativecommons.org/licenses/by-nc-nd/4.0/).

NEW RESEARCH PAPER

Machine Learning-Derived Echocardiographic Phenotypes Predict Heart Failure Incidence in Asymptomatic Individuals

Masatake Kobayashi, MD, PhD,[a,b,*] Olivier Huttin, MD, PhD,[a,b,*] Martin Magnusson, MD, PhD,[c,d,f] João Pedro Ferreira, MD, PhD,[a,b] Erwan Bozec, PhD,[a,b] Anne-Cecile Huby, PhD,[a,b] Gregoire Preud'homme, MSc,[a,b] Kevin Duarte, PhD,[a,b] Zohra Lamiral, MSc,[a,b] Kevin Dalleau, PhD,[e] Emmanuel Bresso, PhD,[e] Malika Smaïl-Tabbone, PhD,[b,e] Marie-Dominique Devignes, PhD,[b,e] Peter M. Nilsson, MD, PhD,[c,g] Margret Leosdottir, MD, PhD,[c,d] Jean-Marc Boivin, MD, PhD,[a,b] Faiez Zannad, MD, PhD,[a,b] Patrick Rossignol, MD, PhD,[a,b] Nicolas Girerd, MD, PhD,[a,b] on behalf of the STANISLAS study

ABSTRACT

OBJECTIVES This study sought to identify homogenous echocardiographic phenotypes in community-based cohorts and assess their association with outcomes.

BACKGROUND Asymptomatic cardiac dysfunction leads to a high risk of long-term cardiovascular morbidity and mortality; however, better echocardiographic classification of asymptomatic individuals remains a challenge.

METHODS Echocardiographic phenotypes were identified using K-means clustering in the first generation of the STANISLAS (Yearly non-invasive follow-up of Health status of Lorraine insured inhabitants) cohort (N = 827; mean age: 60 ± 5 years; men: 48%), and their associations with vascular function and circulating biomarkers were also assessed. These phenotypes were externally validated in the Malmö Preventive Project cohort (N = 1,394; mean age: 67 ± 6 years; men: 70%), and their associations with the composite of cardiovascular mortality (CVM) or heart failure hospitalization (HFH) were assessed as well.

RESULTS Three echocardiographic phenotypes were identified as "mostly normal (MN)" (n = 334), "diastolic changes (D)" (n = 323), and "diastolic changes with structural remodeling (D/S)" (n = 170). The D and D/S phenotypes had similar ages, body mass indices, cardiovascular risk factors, vascular impairments, and diastolic function changes. The D phenotype consisted mainly of women and featured increased levels of inflammatory biomarkers, whereas the D/S phenotype, consisted predominantly of men, displayed the highest values of left ventricular mass, volume, and remodeling biomarkers. The phenotypes were predicted based on a simple algorithm including e′, left ventricular mass and volume (e′VM algorithm). In the Malmö cohort, subgroups derived from e′VM algorithm were significantly associated with a higher risk of CVM and HFH (adjusted HR in the D phenotype = 1.87; 95% CI: 1.04 to 3.37; adjusted HR in the D/S phenotype = 3.02; 95% CI: 1.71 to 5.34).

CONCLUSIONS Among asymptomatic, middle-aged individuals, echocardiographic data-driven classification based on the simple e′VM algorithm identified profiles with different long-term HF risk. (4th Visit at 17 Years of Cohort STANISLAS-Stanislas Ancillary Study ESCIF [STANISLASV4]; NCT01391442) (J Am Coll Cardiol Img 2021;■:■–■) © 2021 The Authors. Published by Elsevier on behalf of the American College of Cardiology Foundation. This is an open access article under the CC BY-NC-ND license (http://creativecommons.org/licenses/by-nc-nd/4.0/).

From the [a]Centre d'Investigations Cliniques Plurithématique 1433, Université de Lorraine, Institut national de la santé et de la recherche médicale 1116, Centre Hospitalier Universitaire Régional de Nancy, France; [b]French Clinical Research Infrastructure Network "Investigation" Network Initiative - Cardiovascular and Renal Clinical Trialists" Cardiovascular and Renal Clinical Trialists Network, France; [c]Department of Clinical Sciences, Lund University, Malmö, Sweden; [d]Department of Cardiology, Skåne

ISSN 1936-878X https://doi.org/10.1016/j.jcmg.2021.07.004

ABBREVIATIONS AND ACRONYMS

DD = diastolic dysfunction

HF = heart failure

HFpEF = heart failure with preserved ejection fraction

LA = left atrial

LV = left ventricular

LVEF = left ventricular ejection fraction

LVH = left ventricular hypertrophy

ML = machine learning

NRI = net reclassification improvement

NT-proBNP = N-terminal pro-B-type natriuretic peptide

TR = tricuspid regurgitation

Asymptomatic left ventricular (LV) systolic dysfunction and ventricular enlargement or hypertrophy are classified under Stage B heart failure (HF), which is characterized by a high risk of developing HF or cardiovascular outcomes (1). Accumulating data have further broadened this category by incorporating LV diastolic dysfunction (DD) (2,3). These structural and functional cardiac alterations may vary with age and comorbidity burden such as hypertension and diabetes mellitus (4–8). Therefore, the inter-relationships of echocardiographic parameters can potentially complicate echocardiogram-based evaluations for identifying high-risk individuals in a populational setting. Indeed, the definition of DD has been a moving target, and several classifications have been proposed over the last 20 years (9–12), leading to large differences in DD prevalence in population-based cohorts (13). Hence, a better use of echocardiographic phenotypes may help identify high-risk individuals and consequently prevent the progression from asymptomatic cardiac abnormalities to overt HF.

Machine learning (ML) clustering provides the potential value of identifying homogeneous groups among populations with heterogeneous underlying features. It has been efficiently used in various cardiovascular settings with noteworthy heterogeneity, eg, early cardiac structure alterations in diabetic patients (14) and patients with HF and preserved ejection fraction (HFpEF) (15). Given that ML clustering can identify groups of individuals with specific characteristics and risk, the relevance of those groups should consequently be apparent by their association with "hard" outcomes including HF onset and death, vascular profiles (associated with adverse cardiac structural and functional remodeling [16,17]) and circulating biomarkers associated with cardiovascular pathophysiology.

The authors hypothesized that echocardiographic phenotypes can be identified using ML-derived decision algorithms in asymptomatic populations and that those phenotypes are associated with different levels of vascular impairments, circulating biomarkers, and a long-term risk for HF. In keeping with the last impairment, the population-based STANISLAS (Yearly non-invasive follow-up of Health status of Lorraine insured inhabitants) cohort provided an opportunity to identify asymptomatic echocardiographic phenotypes and their associations with vascular parameters and proteomic profiles (18). Furthermore, the Malmö Preventive Project cohort provided the additional opportunity of verifying the external validity of this echocardiographic phenotyping by quantifying the association of these echocardiographic phenotypes with a long-term risk of incident HF and cardiovascular death (19).

METHODS

STANISLAS COHORT. The STANISLAS cohort was a single-center familial longitudinal population-based cohort from the Nancy region in France, the features of which have been previously described (18). The cohort, established in 1993 to 1995, enrolled families consisting of 2 parents and at least 2 biological children which were deemed healthy and initially free of declared illness, with the primary objective to investigate gene-gene and gene-environment interactions. Between 2011 and 2015, 1,705 participants underwent the 4th cohort visit. The study was approved by the local ethics committee (Comité de Protection des Personnes Est III-Nancy-France, 11.02.03), and all study participants gave informed consent to participate (NCT01391442).

Collected variables included age, sex, height, weight, smoking status, disease history, medication use, and the following cardiovascular risk factors: hypertension, diabetes mellitus, and dyslipidemia. Hypertension was diagnosed by 3 consecutive office blood pressure measurements or by the use of antihypertensive medication (20).

In the STANISLAS cohort, 701 participants who were initially children were relatively young at the 4th visit (mean age: 34 ± 5 years). As these participants are unlikely to have any echocardiographic abnormalities, only "parents" of the STANISLAS cohort were included in the present analysis. In

University Hospital, Malmö, Sweden; [e]Laboratoire lorrain de Recherche en Informatique et ses Applications, Unité Mixte de Recherche 7503, Université de Lorraine, Vandoeuvre-lès-Nancy, France; [f]Wallenberg Centre for Molecular Medicine, Lund University, Sweden; and the [g]Department of Internal Medicine, Lund University, Skåne University Hospital, Malmö, Sweden. *Drs Kobayashi and Huttin are co-first authors.

The authors attest they are in compliance with human studies committees and animal welfare regulations of the authors' institutions and Food and Drug Administration guidelines, including patient consent where appropriate. For more information, visit the Author Center.

Manuscript received March 2, 2021; revised manuscript received July 1, 2021, accepted July 1, 2021.

addition, participants with a history of HF or missing echocardiographic variables (used in the clustering procedure) were excluded (Supplemental Figure 1).

CARDIAC FUNCTION ANALYSIS IN THE STANISLAS COHORT. Echocardiographic examinations were performed at the Nancy University Hospital Clinical Investigation Center using standard, commercially available ultrasound equipment (Vivid 9, General Electric Medical Systems, Horten, Norway) with a 2.5-MHz phased-array transducer and reviewed on an Echopac workstation version 202 or 203 (GE Healthcare). The measurement of left atrial (LA) volume was obtained from the biplane method of disks (modified Simpson's rule) using apical 4- and 2-chamber views at end-systolic phase (without dedicated LA views maximizing LA size).

Diastolic function was assessed from the mitral inflow pattern by pulsed-wave Doppler. Mitral annular early diastolic velocity (e′) was assessed at the septal and lateral sites of the mitral annulus using tissue Doppler imaging. The E/A ratio, e′ mean, and E/e′ mean ratio were calculated (10). LV systolic deformation was assessed from the 3 apical views with measurement of the global LV systolic strain (GLS %) corresponding to the maximum absolute value of strain derived from strain curves. DD was defined by the 2016 American Society of Echocardiography/European Association of Cardiovascular Imaging recommendations (DD class 2016 assessment with conventional echo variables) (9). The authors also further assessed DD with additional echo biomarkers, complementing the DD 2016 definition with LV hypertrophy (LVH: >95 g/m^2 in women and >115 g/m^2 in men [21]), LV ejection fraction (LVEF) <50% or impaired GLS (>−17.7% in women and >−16.8% in men) (22) as individuals with those abnormalities of cardiac structure or function are likely to have DD as suggested by the latest recommendations (9).

The authors' center's measurement reproducibility by experienced echocardiographers blinded to each other and to demographic parameters has been previously reported (23,24) and is shown in Supplemental Table 1. Overall, intra- and interobserver intraclass correlation coefficients of each echocardiographic parameter provided good reproducibility.

VASCULAR FUNCTION ANALYSIS IN THE STANISLAS COHORT. Central and peripheral blood pressures (BP) and augmentation index were measured using the SphygmoCor cardiovascular management system (AtCor, Sydney, Australia) after arm calibration. Aortic stiffness was evaluated using carotid-to-femoral pulse wave velocity (PWV) assessed using a Complior (Alam Medical) device (25). Intima media thickness (IMT) was measured using a linear probe with an echo-tracking system (Wall Track System [WTS]/ART.LAB) at 1 cm-2 cm below the carotid bifurcation on the right common carotid artery (26). Detailed methods of the PWV and IMT measurements in this cohort have previously been published (27). Total arterial compliance index [= stroke volume/central pulse pressure × body surface area] and systemic vascular resistance index [= 80×mean central pressure/cardiac index] were also assessed based on echocardiographic examinations.

CIRCULATING BIOMARKERS EXPRESSING INFLAMMATION, EXTRACELLULAR MATRIX REMODELING, AND RENAL FUNCTION. Inflammatory mediators associated with diastolic dysfunction in HFpEF were assessed (fatty acid-binding protein [FABP]-4 growth differentiation factor [GDF]-15, and galectin [Gal]-3). Adhesion molecules (vascular cell adhesion molecule [VCAM]-1 and intercellular adhesion molecule [ICAM]-1), transforming growth factor (TGF)β-1, monocyte chemoattractant protein (MCP)-1, receptor for advanced glycosylation end (RAGE) products, interleukin (IL)-6, IL-8, IL-1 receptor-like 2 (IL1RL-2), tumor necrosis factor receptor 1 (TNF-R1), and osteopontin (OPN) were also studied as they were reported to be implicated in the inflammatory process related to HFpEF (28–33).

Extracellular matrix remodeling and angiogenesis in HFpEF were supported by the expression of matrix metalloproteinase (MMP)-1, MMP-2, MMP-9, MMP-12, N-terminal propeptide of procollagen type III (PIIINP), C-terminal propeptide of procollagen type I (PICP), soluble ST-2, N-terminal pro-B-type natriuretic peptide (NT-proBNP), brain natriuretic peptide (BNP), C-type natriuretic peptide (CNP), troponin-I, tissue inhibitor of metalloproteinase (TIMP)-1, TIMP-4, adrenomedullin (ADM), angiogenin (ANG), and vascular endothelial growth factor (VEGF)-A. Blood urea nitrogen (BUN) and creatinine were, furthermore, used to express renal function in HFpEF (34). These selected biomarkers were measured using Proseek (Olink Proteomics, Uppsala, Sweden) multiplex organ damage, metabolism, cardiovascular (CVD) II, III and Inflammation 96 × 96 kits in serum using proximity extension assay technology (35). In addition, PIIINP was measured by using radioimmunoassay (Orion Diagnostica, Eurofins Panlabs) and PICP by enzyme immunoassay (Metra, Quidel Corp.).

MALMÖ PREVENTIVE PROJECT COHORT. The Malmö Preventive Project cohort was a population-based longitudinal cohort of Malmö (Sweden) inhabitants (19). Of 1,792 participants having undergone an echocardiogram from 2002 to 2006, those without a

history of HF were included in our analysis (36). The Lund University's ethics committee (Lund, Sweden) approved the study (LU 244-02), and written informed consent was obtained from each participant. HF hospitalization and other clinical outcomes were retrieved by record linkage between the Swedish personal identification number and national health care databases.

Echocardiograms were conducted using a 3V2c transducer (Acuson Sequoia, AGES-RS and MPP-RES) or an S3 transducer (Sonos 5500 Philips, MPP-RES). According to the recommendations, LV and LA structures, systolic and diastolic function were assessed (37,38). Intra- and interobserver variability and full description of the echocardiographic protocol have previously been reported (36) and are shown in Supplemental Table 1. The values of LV diastolic volume and LA volume were respectively estimated from LV diastolic diameter and LA area based on linear equations derived from the STANISLAS cohort (Supplemental Table 1). DD was coded according to the 2016 American Society of Echocardiography/European Association of Cardiovascular Imaging recommendations. All individuals were considered having a peak tricuspid regurgitation (TR) velocity <2.8 cm/s as this parameter was unavailable. In addition, individuals who had either DD, LVH, or LVEF <50% were also selected.

MACHINE LEARNING APPROACH: CLUSTER ANALYSIS AND DECISION TREE CONSTRUCTION. The Proposed Requirements for Cardiovascular Imaging-Related Machine Learning Evaluation (PRIME) guideline (39) checklist is shown in Supplemental Table 2.

Cluster analysis was performed based on echocardiographic data (ie, LV mass index [LVMi], LV end-diastolic volume index [LVEDVi], LA volume index [LAVi], LVEF, GLS, E/A ratio, e′ mean, and E/e′ mean ratio).

K-means clustering analysis was performed to identify echocardiographic patterns using the K-means R program. Cluster analysis was performed on standardized values (mean = 0; SD = 1), based on the Euclidean distance as the dissimilarity metric. This algorithm aimed at finding clusters by: 1) initializing k points as the centroids; 2) assigning each data point to the closest centroid; and 3) recomputing the coordinates of the k centroids as the barycenters of the new clusters. This procedure was repeated until the centroids were stable. A total of 30 different quality measurements for different numbers of clusters were used to find the optimal number of clusters using the NbClust R program. Missing values were not imputed. In order to choose between available clustering methods, the same echocardiographic parameters were used in a hierarchical clustering and latent class model (LCM) clustering. K-means clustering achieved a higher internal consistency than the hierarchical clustering after cluster bootstrap (×1,000) but provided consistent results with the LCM approach (Supplemental Table 3). Thus, the authors reported the results of the K-means clustering as the primary analysis.

Decision trees provided parsimonious and transparent rules that were particularly appropriate in producing a hierarchy of 2 or more predictive factors simultaneously. Each patient in the data set (or the cohort) was labeled with a corresponding cluster. Decision trees were subsequently constructed to predict the clusters by using the rpart R program (40). This program selected the best threshold of each echocardiographic parameter to maximize the discrimination of clusters and evaluated through a 10-fold cross-validation to ensure that the prediction error was correctly estimated.

The overall accuracy of these cluster predictions was, furthermore, explored using random forest classification using the random Forest R application (41). Parameters of the random forest were optimized by a grid search with the Caret R package (42) by varying the number of trees between 50 and 1000, and modifying the number of selected variables to construct each split from 2 to the total number of available variables. Retained parameters were 500 trees and 15 random selected variables and the final model accuracy was evaluated by a 10-fold cross validation.

Principal component analysis was used to visualize the relationship between echocardiographic parameters used in cluster analysis and individuals in each echocardiographic phenotype.

The source code of all analyses performed within this project including the random forest model is available in GitLab.

STATISTICAL ANALYSIS. Categorical variables are described as frequencies (percentages), whereas continuous variables are described as mean ± SD or median interquartile ranges (IQR: 25th, 75th percentiles) depending on variable distributions. Comparisons of participant characteristics across echocardiographic phenotypes were analyzed using analysis of variance (ANOVA), Kruskal-Wallis, and chi-squared tests, as appropriate. Given the number of circulating biomarkers in the STANISLAS cohort, comparisons were analyzed using Kruskal-Wallis tests followed by p values corrected for the multiplicity of tests, using the Benjamini Hochberg method.

TABLE 1 Clinical and Vascular Characteristics According to Echocardiographic Phenotypes in the STANISLAS Cohort

	Global (N = 827)	MN Phenotype (n = 334)	D Phenotype (n = 323)	D/S Phenotype (n = 170)	*P* Value	*P* Value for the Comparison Between D and D/S Phenotypes
Age, yrs	60.0 ± 5.0	59.0 ± 4.0	61.0 ± 5.0	61.0 ± 5.0	**<0.001**	0.11
Men	399.0 (48.2)	143.0 (42.8)	128.0 (39.6)	128.0 (75.3)	**<0.001**	**<0.001**
Body mass index, kg/m^2	27.0 ± 4.0	25.0 ± 4.0	27.0 ± 4.0	28.0 ± 5.0	**<0.001**	0.12
Medical history						
Hypertension	234.0 (28.3)	59.0 (17.7)	115.0 (35.6)	60.0 (35.3)	**<0.001**	0.95
Diabetes	44.0 (5.4)	13.0 (3.9)	20.0 (6.3)	11.0 (6.5)	0.31	0.93
Dyslipidemia	259.0 (31.3)	81.0 (24.3)	118.0 (36.5)	60.0 (35.3)	**0.001**	0.79
Coronary artery disease	20.0 (2.4)	7.0 (2.1)	6.0 (1.9)	7.0 (4.1)	0.27	0.15
Smoking	101 (12.3)	42 (12.7)	45 (14.2)	14 (8.2)	0.16	0.06
Medications						
Antihypertensive treatment	225.0 (27.5)	58.0 (17.5)	104.0 (32.6)	63.0 (37.7)	**<0.001**	0.26
Statin	156.0 (18.9)	40.0 (12.0)	76.0 (23.5)	40.0 (23.5)	**<0.001**	0.99
ACC/AHA Heart Failure Stage						
Stage 0	398.0 (48.1)	216.0 (64.7)	151.0 (46.7)	31.0 (18.2)	**<0.001**	0.81
Stage A	247.0 (29.9)	75.0 (22.5)	141.0 (43.7)	31.0 (18.2)		
Stage B	182.0 (22.0)	43.0 (12.9)	31.0 (9.6)	108.0 (63.5)		
Biochemistry						
HbA1c, %	5.8 ± 0.6	5.7 ± 0.5	5.8 ± 0.6	5.8 ± 0.6	**0.008**	0.30
Total cholesterol, mg/dL	224.0 ± 38.0	225.0 ± 37.0	227.0 ± 39.0	218.0 ± 38.0	0.053	**0.02**
LDL cholesterol, mg/dL	142.0 ± 34.0	144.0 ± 33.0	143.0 ± 35.0	138.0 ± 34.0	0.25	0.31
eGFR, ml/min/1.73m^2	91.0 ± 17.0	91.0 ± 16.0	91.0 ± 17.0	93.0 ± 17.0	0.48	0.18
Vascular parameters						
Heart rate, beats/min	62.0 ± 8.0	61.0 ± 8.0	63.0 ± 9.0	60.0 ± 8.0	**<0.001**	**<0.001**
Peripheral SP, mm Hg	124.0 ± 17.0	119.0 ± 15.0	126 ± 17	130 ± 18	**<0.001**	**0.044**
Central SP, mm Hg	115.0 ± 17.0	110.0 ± 16.0	117.0 ± 17.0	119.0 ± 18.0	**<0.001**	0.48
Peripheral AI, %	85.0 ± 17.0	85.0 ± 17.0	86.0 ± 17.0	82.0 ± 14.0	0.11	**0.01**
Central AI, %	34.0 ± 12.0	34.0 ± 11.0	35.0 ± 12.0	34.0 ± 13.0	0.30	0.29
IMT, µm	691.0 (616.0-784.0)	673.0 (598.0-764.0)	689.0 (627.0-771.0)	738.0 (656.0-822.0)	**<0.001**	**<0.001**
PWV, m/s	8.4 (7.5-9.4)	8.1 (7.3-9.0)	8.6 (7.7-9.6)	8.7 (7.6-9)	**<0.001**	0.56
TAC index, ml/mm Hg/m^2	1.00 (0.79-1.25)	1.06 (0.88-1.32)	0.95 (0.73-1.17)	1.01 (0.77-1.33)	**<0.001**	**0.03**
SVR index, dyne x s/cm^5/m^2	2,624.0 (2,254.0-3,148.0)	2,568.0 (2,237.0-3,007.0)	2,648.0 (2,299.0-3,235.0)	2,724.0 (2,223.0-3,360.0)	**0.021**	0.83

Values are mean ± SD, n (%), or median interquartile range (25th, 75th percentile). **Bold** values indicate statistical significance.

ACC/AHA = American College of Cardiology/American Heart Association; AI = augmentation index; D = diastolic changes; D/S = diastolic changes with structural remodeling; eGFR = estimated glomerular filtration rate; HbA1c = glycosylated hemoglobin; IMT = intima media thickness; IQR = interquartile range; LDL = low-density lipoprotein; PWV = pulse wave velocity; SP = systolic pressure; STANISLAS = Yearly non-invasive follow-up of Health status of Lorraine insured inhabitants; SVR = systemic vascular resistance; TAC = total arterial compliance.

In the Malmö cohort, primary outcome was a composite of initial hospitalization for HF or cardiovascular death. Secondary outcome was a composite of cardiovascular mortality and hospitalization (HF, arrhythmia, or coronary artery disease). Survival probabilities were estimated using the Kaplan-Meier method. Cox proportional-hazards models for echocardiographic phenotypes were used to obtain unadjusted and covariate adjusted HRs. The covariates used for adjustments were Model 1: Heart OMics in Aging HF risk score (without creatinine) plus cystatin-C and NT-proBNP (43); Model 2: adjusted for ARIC (Atherosclerosis Risk In Communities) HF risk score without NT-proBNP; and Model 3: ARIC HF risk score plus NT-proBNP (44). The increased C index and net reclassification improvement (NRI) were implemented to assess added prognostic values of echocardiographic phenotypes for the primary outcome on top of: 1) ARIC HF risk score plus NT-proBNP; 2) cardiac structure and function abnormalities (ie, LVH, LAVi >34 ml/m^2, septal e′ <7 cm/s or lateral e′ <10 cm/s, E/e′ mean >14); 3) DD class 2016 assessment with conventional echo variables; and 4) DD class 2016 assessment with additional echo biomarkers.

All statistical analyses were performed using R version 3.4.0 software (R Development Core Team. A *P* value <0.05 was considered statistically significant.

RESULTS

Participants with missing values of at least 1 echocardiographic parameter used in cluster analysis were excluded (Supplemental Table 4). Those individuals

TABLE 2 Echocardiographic Characteristics According to Echocardiographic Phenotypes in the STANISLAS Cohort

	Global (N = 827)	MN Phenotype (n = 334)	D Phenotype (n = 323)	D/S Phenotype (n = 170)	*P* Value	*P* Value for the Comparison Between D and D/S Phenotypes
LV structure						
LVEDD, cm	4.5 ± 0.5	4.4 ± 0.5	4.4 ± 0.5	4.9 ± 0.5	**<0.001**	**<0.001**
LVEDVi, ml/m^2	48.0 ± 13.0	49.0 ± 11.0	41.0 ± 9.0	60.0 ± 14.0	**<0.001**	**<0.001**
LVEDVi >74 ml/m^2 in men or LVEDVi >61 ml/m^2 in women	56.0 (6.8)	18.0 (5.4)	1.0 (0.3)	37.0 (21.8)	**<0.001**	**<0.001**
LVMi, g/m^2	80.0 ± 19.0	73.0 ± 15.0	76.0 ± 14.0	100.0 ± 19.0	**<0.001**	**<0.001**
Men	86.0 ± 19.0	78.0 ± 15.0	79.0 ± 13.0	102.0 ± 19.0	**<0.001**	**<0.001**
Women	73.0 ± 16.0	69.0 ± 14.0	73.0 ± 15.0	95.0 ± 18.0	**<0.001**	**<0.001**
LVMi >115 ml/m^2 in men or LVMi >95 ml/m^2 in women	80.0 (9.7)	10.0 (3.0)	18.0 (5.6)	52.0 (30.6)	**<0.001**	**<0.001**
RWT	0.41 ± 0.09	0.40 ± 0.08	0.41 ± 0.09	0.42 ± 0.10	**0.017**	0.38
RWT >0.42	337.0 (40.7)	123.0 (36.8)	137.0 (42.4)	77.0 (45.3)	0.14	0.54
LV geometry						
Normal	456.0 (55.1)	209.0 (62.6)	180.0 (55.7)	67.0 (39.4)	**<0.001**	0.68
Concentric remodeling	291.0 (35.2)	115.0 (34.4)	125.0 (38.7)	51.0 (30.0)		
Concentric hypertrophy	46.0 (5.6)	8.0 (2.4)	12.0 (3.7)	26.0 (15.3)		
Eccentric hypertrophy	34.0 (4.1)	2.0 (0.6)	6.0 (1.9)	26.0 (15.3)		
LA structure						
LA area, cm^2	16.0 ± 4.0	16.0 ± 3.0	16.0 ± 3.0	19.0 ± 4.0	**<0.001**	**<0.001**
LAVi, ml/m^2	23.0 ± 8.0	22.0 ± 7.0	22.0 ± 6.0	29.0 ± 8.0	**<0.001**	**<0.001**
LAVi >34 ml/m^2	75.0 (9.1)	15.0 (4.5)	12.0 (3.7)	48.0 (28.2)	**<0.001**	**<0.001**
LV systolic function						
LVEF %	66.0 ± 6.0	67.0 ± 6.0	67.0 ± 6.0	62.0 ± 7.0	**<0.001**	**0.001**
LVEF <50%	10.0 (1.2)	0.0 (0.0)	0.0 (0.0)	10.0 (5.9)	**<0.001**	0.97
GLS %	−21.0 ± 3.0	−22.0 ± 3.0	−20.0 ± 3.0	−19.0 ± 3.0	**<0.001**	**<0.001**
GLS >−16.8% in men or GLS >−17.7% in women	97.0 (11.7)	11.0 (3.3)	43.0 (13.3)	43.0 (25.3)	**<0.001**	**<0.001**
LV diastolic function						
E wave, cm/s	65.0 ± 13.0	68.0 ± 13.0	66.0 ± 13.0	59.0 ± 12.0	**<0.001**	**<0.001**
A wave, cm/s	69.0 ± 16.0	62.0 ± 15.0	76.0 ± 16.0	68.0 ± 13.0	**<0.001**	**<0.001**
E/A ratio	1.0 ± 0.3	1.1 ± 0.3	0.9 ± 0.2	0.9 ± 0.2	**<0.001**	0.60
e′ mean, cm/s	9.6 ± 2.0	11.2 ± 1.4	8.3 ± 1.2	8.7 ± 1.7	**<0.001**	**0.002**
e′ septal <7 cm/s or e′ lateral <10 cm/s	378.0 (45.7)	28.0 (8.4)	249.0 (77.1)	101.0 (59.4)	**<0.001**	**<0.001**
E/e′ mean	7.1 ± 1.8	6.1 ± 1.2	8.1 ± 1.8	7.0 ± 1.8	**<0.001**	**<0.001**
E/e′ mean <14	7.0 (0.8)	0.0 (0.0)	4.0 (1.2)	1.0 (0.6)	0.12	0.50
S/D ratio (N = 659)	1.4 ± 0.4	1.4 ± 0.4	1.4 ± 0.5	1.4 ± 0.5	0.40	0.43
Peak TR velocity, cm/s (N = 463)	2.18 ± 0.35	2.18 ± 0.36	2.17 ± 0.36	2.22 ± 0.31	0.53	0.61
peak TR velocity>2.8 cm/s (N = 463)	6.0 (1.3)	3.0 (1.4)	0.0 (0.0)	3.0 (3.0)	0.12	0.98
DD class 2016 assessment with conventional echo variables					**<0.001**	**<0.001**
Normal	777.0 (94.7)	332.0 (99.4)	309.0 (95.7)	136.0 (80.0)		
Indeterminate	40.0 (5.2)	2.0 (0.6)	14.0 (4.3)	24.0 (14.1)		
Diastolic dysfunction	10.0 (1.2)	0.0 (0.0)	0.0 (0.0)	10.0 (5.9)		
DD class 2016 assessment with additional echo biomarkers[a]	166.0 (20.1)	19.0 (5.7)	61.0 (18.9)	86.0 (50.6)	**<0.001**	**<0.001**

Values are mean ± SD or n (%). [a]This variable was defined by a composite of DD class 2016 assessment with conventional echo variables, left ventricular hypertrophy (>95 g/m^2 in women and >115 g/m^2 in men) and/or LVEF <50% or impaired GLS (>−17.7% in women and >−16.8% in men). **Bold** values indicate statistical significance.

D = diastolic changes; D/S = diastolic changes with structural remodeling; DD = diastolic dysfunction; E/A = ratio of peak early and late diastolic velocities; E/e′ ratio = ratio of early mitral inflow velocity and mitral annular early diastolic velocity; e′ mean = mean value of early diastolic velocity at the septal and lateral sites of the mitral annulus; GLS = global longitudinal strain; IQR = interquartile range; LAVi = left atrial volume index; LVEDD = left ventricular end-diastolic diameter; LVEDVi = left ventricular end-diastolic volume index; LVEF = left ventricular ejection fraction; LVMi = left ventricular mass index; MN = mostly normal; RWT = relative wall thickness; S/D = ratio of pulmonary vein peak systolic velocity and peak diastolic velocity; STANISLAS = Suivi Temporaire Annuel Non-Invasif de la Santé des Lorrains Assurés Sociaux; TR = tricuspid regurgitation.

more often had comorbidities (eg, obesity, hypertension, diabetes) than those with complete echocardiographic data. In a total of 827 participants included in the current analysis 60 ± 5 years (48.2% men), mean body mass index was 27 kg/m^2, 28.3% of participants had hypertension, 5.4% had diabetes mellitus, and mean LVEF was 66% (Tables 1 and 2).

In the Malmö Preventive Project Cohort, a total of 1,394 participants were included (Table 3). Age was 67 ± 6 years, 70.0% of participants were men, mean body mass index was 28 kg/m^2, 63.7% had hypertension, and 34.3% had diabetes mellitus.

CLUSTERS DERIVED FROM ECHOCARDIOGRAPHIC DATA. The present cluster analysis identified 3

TABLE 3 Baseline Characteristics According to the Echocardiographic Phenotypes Predicted by the e′VM Algorithm in the Malmö Cohort

	Global (N = 1,394)	MN Phenotype (n = 440)	D Phenotype (n = 512)	D/S Phenotype (n = 442)	*P* Value	*P* Value for the Comparison Between D and D/S Phenotypes
Age, yrs	67.0 ± 6.0	63.0 ± 5.0	69.0 ± 5.0	69.0 ± 5.0	**<0.001**	0.39
Men	976.0 (70.0)	353.0 (80.2)	229.0 (44.7)	394.0 (89.1)	**<0.001**	**<0.001**
Body mass index, kg/m^2	28.0 ± 4.0	28.0 ± 4.0	28.0 ± 4.0	28.0 ± 4.0	0.27	0.96
Medical history						
Hypertension	887.0 (63.7)	251.0 (57.2)	327.0 (64.0)	309.0 (69.9)	**<0.001**	0.053
Diabetes	475.0 (34.3)	125.0 (28.4)	169.0 (33.5)	181.0 (41.2)	**<0.001**	**0.014**
Coronary artery disease	76.0 (5.5)	21.0 (4.8)	18.0 (3.5)	37.0 (8.4)	**0.003**	**0.002**
Atrial fibrillation	45.0 (3.2)	17.0 (3.9)	15.0 (2.9)	13.0 (2.9)	0.66	0.99
Smoking	245.0 (17.6)	91.0 (20.7)	72.0 (14.1)	82.0 (18.6)	**0.023**	0.06
Systolic BP, mm Hg	148.0 ± 20.0	145.0 ± 19.0	146.0 ± 19.0	152.0 ± 21.0	**<0.001**	**<0.001**
Diastolic BP, mm Hg	85.0 ± 10.0	84.0 ± 9.0	84.0 ± 10.0	86.0 ± 11.0	**0.02**	**0.03**
Heart rate, beat/min	71.0 ± 12.0	71.0 ± 12.0	74.0 ± 12.0	68.0 ± 11.0	**<0.001**	**<0.001**
Biochemistry						
Blood glucose, mg/dL	122.0 ± 37.0	120.0 ± 30.0	119.0 ± 36.0	128.0 ± 42.0	**<0.001**	**<0.001**
Triglyceride, mg/dL	129.0 ± 83.0	128.0 ± 92.0	130.0 ± 76.0	128.0 ± 82.0	0.93	0.54
HDL Cholesterol, mg/dL	52.0 ± 16.0	51.0 ± 16.0	55.0 ± 17.0	49.0 ± 14.0	**<0.001**	**<0.001**
LDL Cholesterol, mg/dL	137.0 ± 39.0	138.0 ± 40.0	138.0 ± 40.0	134.0 ± 38.0	0.14	0.06
Cystatin C, mg/L	1.05 (0.95-1.18)	1.02 (0.94-1.13)	1.07 (0.95-1.21)	1.08 (0.95-1.23)	**<0.001**	0.45
NT-proBNP, pg/mL	11 (6-21)	7 (5-14)	13 (7-23)	15 (7-32)	**<0.001**	**0.002**
Echocardiographic parameters						
LVEDD, cm	4.8 ± 0.5	4.8 ± 0.5	4.5 ± 0.4	5.0 ± 0.5	**<0.001**	**<0.001**
LVEF, %	62.0 ± 5.0	60.0 ± 4.0	63.0 ± 6.0	62.0 ± 6.0	**<0.001**	**<0.001**
LVMi, g/m^2	89.0 ± 22.0	83.0 ± 18.0	77.0 ± 13.0	109.0 ± 22.0	**<0.001**	**<0.001**
Men	92.0 ± 23.0	85.0 ± 18.0	75.0 ± 11.0	108.0 ± 22.0	**<0.001**	**<0.001**
Women	83.0 ± 20.0	76.0 ± 15.0	80.0 ± 14.0	119.0 ± 16.0	**<0.001**	**<0.001**
LA area, cm^2	20.0 ± 4.0	20.0 ± 4.0	19.0 ± 4.0	21.0 ± 4.0	**<0.001**	**<0.001**
E/A ratio	0.9 ± 0.3	1.0 ± 0.3	0.9 ± 0.2	0.9 ± 0.3	**<0.001**	0.19
e′ mean, cm/s	8.8 ± 2.8	12.1 ± 1.7	7.3 ± 1.6	7.1 ± 1.7	**<0.001**	**0.043**
E/e′ mean	9.1 ± 3.6	6.2 ± 1.4	10.3 ± 3.4	10.5 ± 3.8	**<0.001**	0.89
DD class 2016 assessment with conventional echo variables					**<0.001**	**<0.001**
Normal	1,183.0 (84.9)	439.0 (99.8)	414.0 (80.9)	330.0 (74.7)		
Indeterminate	174.0 (12.5)	1.0 (0.2)	84.0 (16.4)	89.0 (20.1)		
Diastolic dysfunction	37.0 (2.7)	0.0 (0.0)	14.0 (2.7)	23.0 (5.2)		
DD class 2016 assessment with additional echo biomarkers[a]	265.0 (19.0)	32.0 (7.3)	56.0 (10.9)	177.0 (40.0)	**<0.001**	**<0.001**

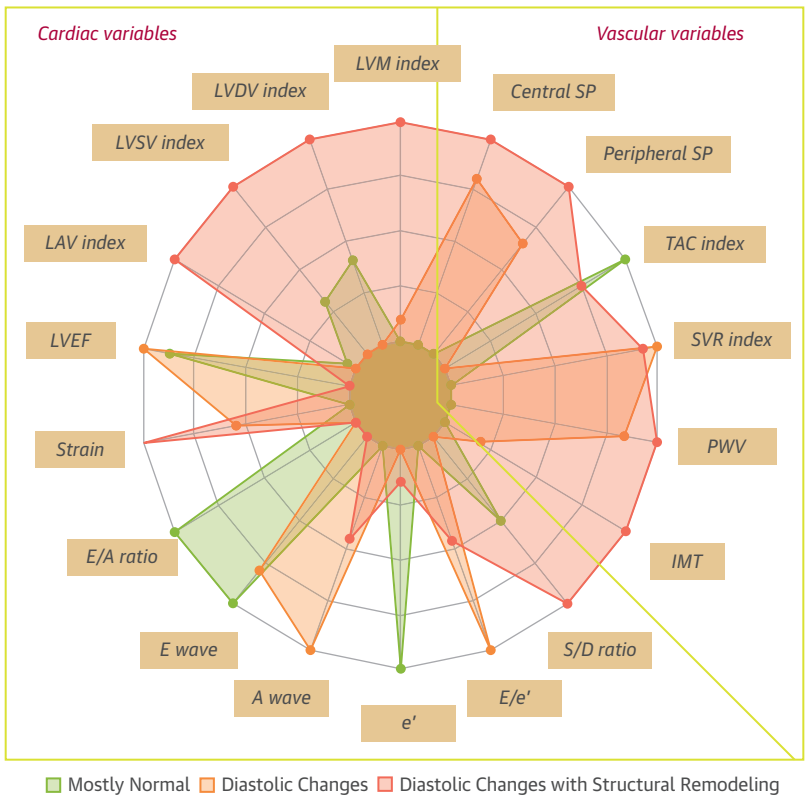
Values are mean ± SD, n (%), or median IQR (25th, 75th percentile). [a]This variable was defined by a composite of diastolic dysfunction class 2016 assessment with conventional echo variables, left ventricular hypertrophy (>95 g/m^2 in women and >115 g/m^2 in men) and/or left ventricular ejection fraction <50%. **Bold** values indicate statistical significance.

NT-proBNP = N-terminal pro-B-type natriuretic peptide; other abbreviations are as in Tables 1 and 2.

groups with different echocardiographic phenotypes (**Tables 1 and 2, Figure 1,** Supplemental Figure 2). The largest cluster (n = 334), labeled mostly normal (MN) phenotype, had the highest e′ and E/A ratio and the highest (absolute) LV systolic strain. The next largest cluster (n = 323), labeled "diastolic changes (D)" phenotype, had lower e′ and higher E/e′ ratio. The last cluster (n = 170), labeled "diastolic changes with structural remodeling (D/S)" phenotype, had the highest LV mass and volumes, highest LA volume, and lowest (absolute) LV systolic strain as well as lower e′ and higher E/e′ ratio. The prevalence of DD class 2016 assessment with conventional echo variables was very low in all 3 phenotypes (<5%), and approximately one-half of individuals with D/S phenotype had DD class 2016 assessment with additional echo biomarkers (**Table 2**).

Participant characteristics according to hierarchical clustering-derived echocardiographic phenotypes are presented, and similar patterns of echocardiographic phenotypes were observed between K-means clustering and hierarchical clustering (Supplemental Table 5, Supplemental Figure 3). In addition, the LCM approach provided the consistent phenotypes with the K-means clustering (Randal index: 0.83) (Supplemental Table 3).

FIGURE 1 **Radar Chart of Cardiovascular Parameters across Echocardiographic Phenotypes in the STANISLAS Cohort**



Radar charts illustrate the differences in cardiac/vascular parameters across the 3 echocardiographic phenotypes. The points most distant from the center indicate higher values. The "diastolic changes" phenotype expressed lower e′ and higher E/e′ ratio, and the "diastolic changes with structural remodeling" phenotype displayed the highest left ventricular mass and volume and left atrial volume as well as lower e′ and higher E/e′ ratio. Similar impairments in vascular function were observed between these 2 phenotypes. E/A = ratio of peak early and late diastolic velocities; IMT = intima media thickness; LAV = left atrial volume; LVDV = left ventricule diastolic volume; LVEF = left ventricular ejection fraction; LVM = left ventricular mass; LVSV = left ventricule stroke volume; PWV = pulse wave velocity; S/D = ratio of pulmonary vein peak systolic velocity and peak diastolic velocity; SP = systolic pressure; SVR = systemic vascular resistance; TAC = total arterial compliance.

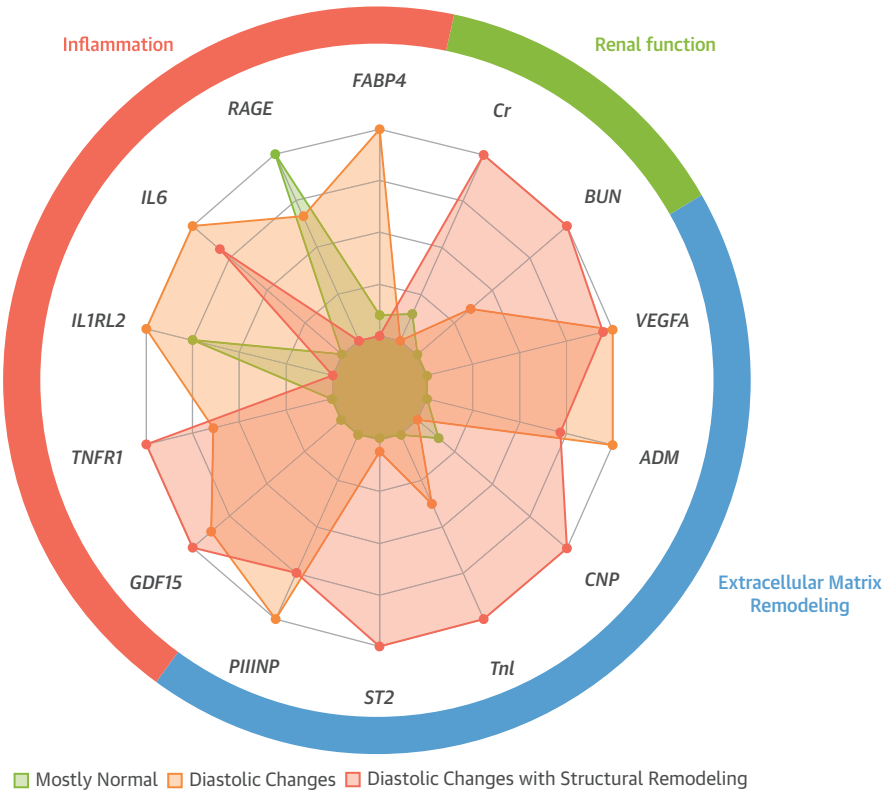
When performing cluster analysis separately in men and women, similar patterns of echocardiographic phenotypes (ie, phenotypes D and D/S) were observed (Supplemental Figure 3).

CLINICAL CHARACTERISTICS ACCORDING TO ECHOCARDIOGRAPHIC PHENOTYPES IN THE STANISLAS COHORT. The D phenotype consisted mainly of women, whereas the D/S phenotype included predominantly of men. The D and D/S phenotypes exhibited older age, higher body mass index, and more often cardiovascular risk factors than the MN phenotype; however, no significant differences among these clinical features were observed between D and D/S phenotypes (Table 1).

VASCULAR PROFILES ACCORDING TO ECHOCARDIOGRAPHIC PHENOTYPES IN THE STANISLAS COHORT. The MN phenotype had more favorable levels of central and peripheral pressure and vascular stiffness (PWV and IMT) than the D and D/S phenotypes, whereas no significant differences were observed between the D and D/S phenotypes (PWV [m/s], 8.6 [95% CI: 7.7 to 9.6] in D phenotype vs 8.7 [95% CI: 7.6 to 9.8] in D/S phenotype; $P = 0.56$]) (Table 1, Figure 1).

CIRCULATING BIOMARKERS ACCORDING TO ECHOCARDIOGRAPHIC PHENOTYPES IN THE STANISLAS COHORT. Of the 32 circulating biomarkers, 14 were significantly different across the 3 phenotypes. These

FIGURE 2 **Radar Chart of Circulating Biomarkers Across Echocardiographic Phenotypes in the Stanislas Cohort**



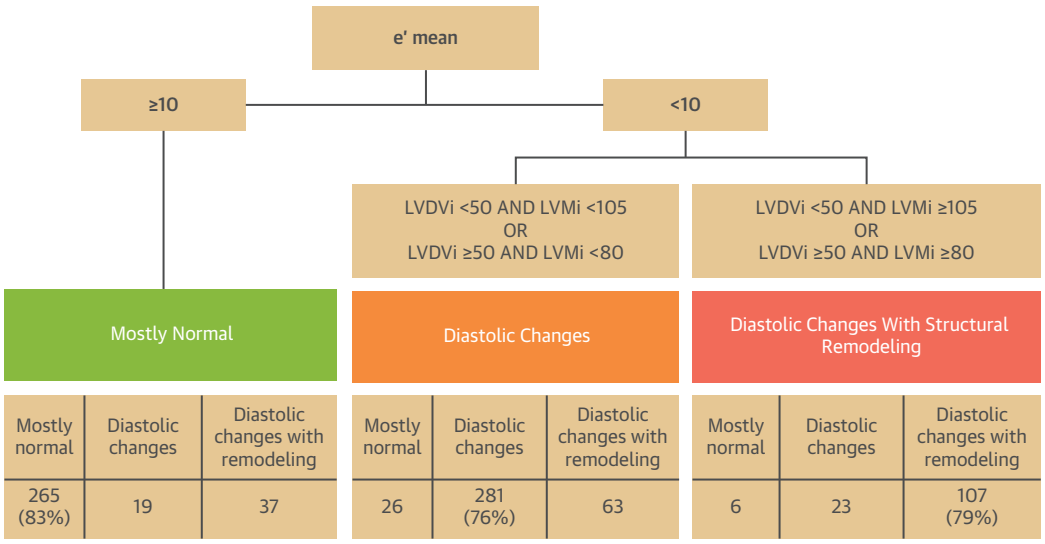
Overall, the "diastolic changes" phenotype exhibited higher levels of inflammatory biomarkers, whereas the "diastolic changes with structural remodeling" phenotype expressed increased levels of remodeling biomarkers. ADM = adrenomedullin; BUN = blood urea nitrogen; CNP = C-type natriuretic peptide; Cr = creatinine; FABP4 = fatty acid binding protein 4; GDF15 = Growth Differentiation Factor 15; IL1RL2 = Interleukin 1 Receptor Like 2; IL6 = Interleukin 6; PIIINP = propeptide of procollagen type III; RAGE = receptor for advanced glycosylation end; ST2 = soluble interleukin 2; TNFR1 = Tumor necrosis factor receptor 1; TnI = troponin I; VEGFA = vascular endothelial growth factor A.

biomarkers were associated with different pathophysiological domains (ie, inflammation and extracellular matrix remodeling) (**Figure 2,** Supplemental Table 6). Overall, the D phenotype exhibited the highest levels of circulating biomarkers associated with inflammation (ie, FABP4, IL-6, and IL1RL2). Markers generally associated with remodeling (ie, GDF15, PIIINP, ST-2, troponin-I, and CNP, increased from the MN to the D and D/S phenotypes, with the highest ST-2, troponin-I, and CNP values observed in the D/S phenotype.

DECISION TREE AND RANDOM FOREST TO IDENTIFY ECHOCARDIOGRAPHIC PHENOTYPES IN THE STANISLAS COHORT: "e′VM" ALGORITHM. The decision tree identified mean e′, LVEDVi, and LVMi as the most relevant variables to correctly classify participants in 1 of the echocardiographic profiles. The global accuracy of the decision tree was good (79.0%) (**Figure 3**). Addition of clinical variables (ie, age, sex, body mass index, prevalence of hypertension, diabetes, dyslipidemia, coronary artery disease, and smoking) to the candidate variables for decision tree building did not modify the decision algorithm; hence, these clinical variables were not retained by the algorithm as relevant additions to the decision tree. In the following sections, the authors refer to the constructed decision tree as the "e′VM" algorithm. Furthermore, the random forest classifier (available at Gitlab software) for these echocardiographic phenogroups provided an overall accuracy of 0.86.

EXTERNAL VALIDATION OF e′VM ALGORITHM IN THE MALMÖ PREVENTIVE PROJECT COHORT. Participant characteristics according to e′VM algorithm phenotypes in the Malmö cohort are presented in **Table 3**. The MN phenotype (n = 440) displayed the most favorable values of clinical, biological, and echocardiographic profiles. The D phenotype

FIGURE 3 e′VM Algorithm for Echocardiographic Phenotypes Using the Decision Tree From the STANISLAS Cohort Data



An algorithm based on mean e′, left ventricular volume, and mass enabled classifying asymptomatic individuals into echocardiography-phenotypic subgroups with a high accuracy. LVDVi = LVDV = left ventricule diastolic volume index; LVMi = left ventricular mass index; STANISLAS = Yearly non-invasive follow-up of Health status of Lorraine insured inhabitants.

included 512 participants and displayed the lowest proportion of men, whereas the D/S phenotype (n = 442) featured a high proportion of men, the highest NT-proBNP level, and the largest LV mass and LA surface area indices. Similar age, body mass index, cardiovascular risk factors and diseases (ie, hypertension, dyslipidemia and renal function) and diastolic function alterations were observed in the D and D/S phenotypes (**Table 3**).

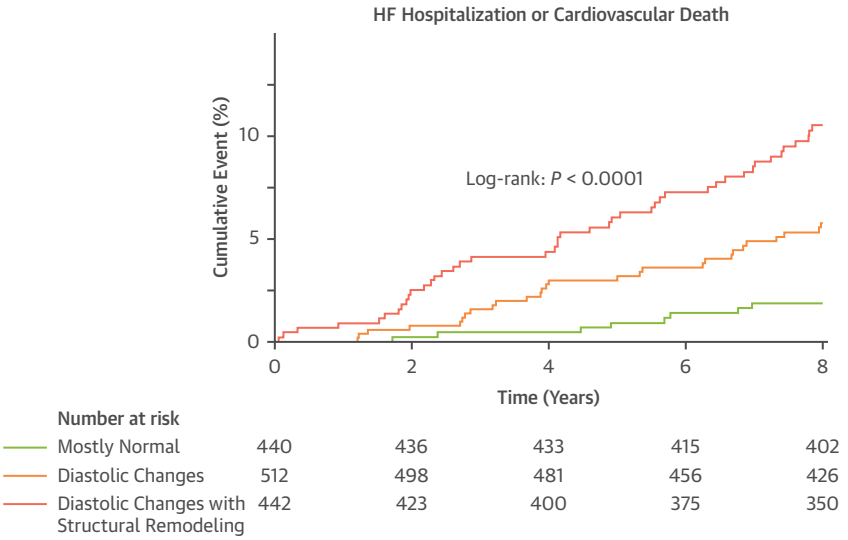
SURVIVAL ANALYSIS IN THE Malmö Preventive Project Cohort. In the Malmö study, during a median follow-up of 10.3 years (9.8 to 11.1 years), 10.1% of participants met the primary outcome. Compared with the MN phenotype, both the D and D/S phenotypes were significantly associated with increased rates of the primary outcome (crude HR: 2.47; 95% CI: 1.38 to 4.41; $P = 0.002$ for the D phenotype and crude HR: 4.67; 95% CI: 2.67 to 8.14; $P < 0.001$ for the D/S phenotype) (**Figure 4,** Supplemental Table 7). After adjustment for the ARIC HF risk score plus NT-proBNP, the D and D/S phenotypes remained significantly associated with the primary outcome (adjusted HR: 1.87; 95% CI = 1.04 to 3.37; $P = 0.03$ for the D phenotype and adjusted HR: 3.02; 95% CI: 1.71 to 5.34; $P < 0.001$ for the D/S phenotype). Poor prognosis of the D/S phenotype persisted even in terms of the composite of cardiovascular hospitalization and mortality (Supplemental Table 7).

Echocardiographic phenotypes significantly improved prognostic performance on top of the ARIC HF risk score (increased C-index: 3.7; 95% CI = 1.3 to 6.1; $P = 0.002$; NRI: 33.3; 95% CI = 0.3 to 55.0; $P = 0.049$). Furthermore, the discriminative values of these echocardiographic phenotypes were consistently observed on top of traditionally defined cardiac structure or function abnormalities (Supplemental Table 8).

DISCUSSION

The present analysis enabled identifying 3 echocardiographic phenotypes with differential biological characteristics and risk of HF, namely, "mostly normal (MN)," "diastolic changes," and "diastolic changes with structural remodeling" phenotypes (**Central Illustration**). The D phenotype had the most abnormal diastolic function parameters and typically exhibited higher levels of inflammatory biomarkers, whereas the D/S phenotype expressed LV and LA remodeling as well as diastolic changes and was associated with higher levels of extracellular matrix remodeling. Both phenotypes were associated with vascular impairments as well as a higher risk of HF hospitalization and/or cardiovascular mortality. Our findings suggest that the easy-to-use e′VM echocardiographic-based algorithm presented herein may identify asymptomatic individuals with a higher

FIGURE 4 **Risk of Initial Heart Failure Hospitalization or Cardiovascular Death According to Echocardiographic Phenotypes Using the e′VM Algorithm in the Malmö Cohort**



The "diastolic changes" and "diastolic changes with structural remodeling" phenotypes were associated with a higher risk of the composite of cardiovascular mortality and/or heart failure hospitalization. HF = heart failure.

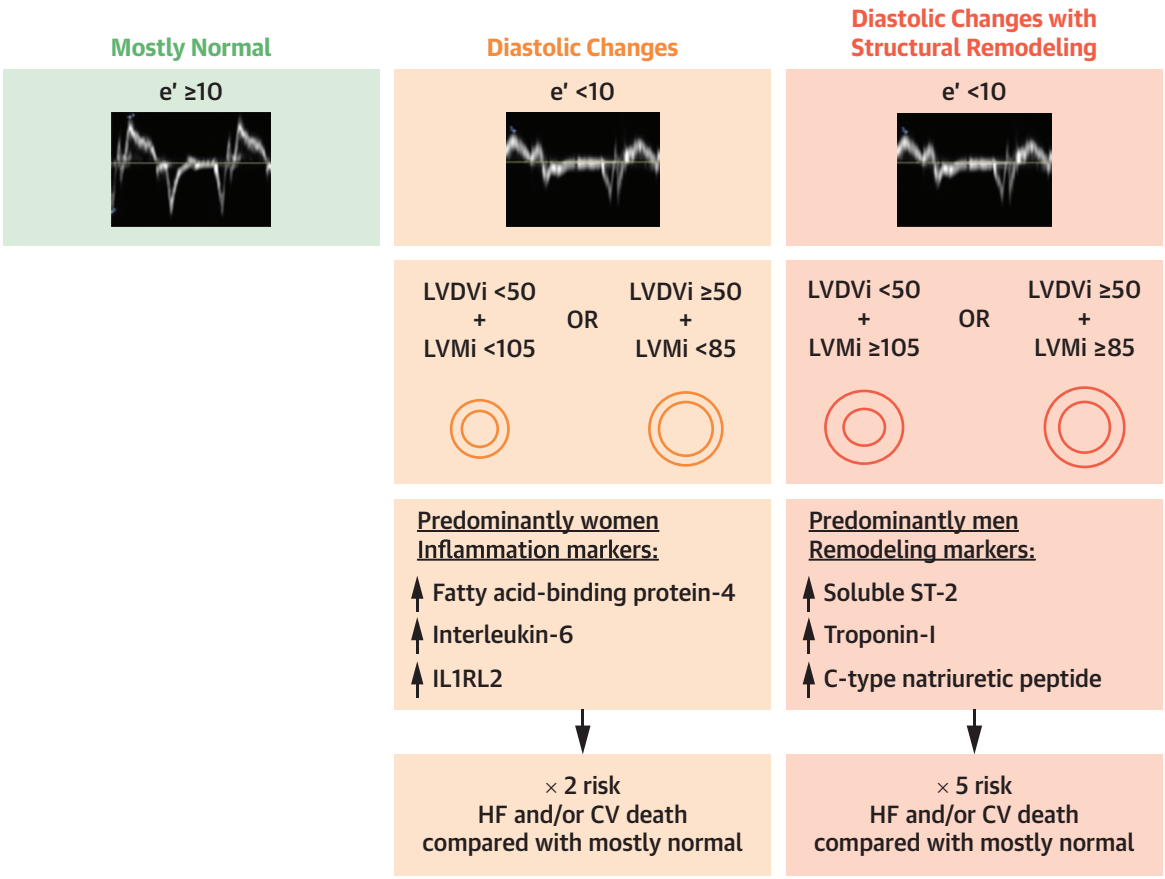
risk of developing HF or cardiovascular death. Importantly, this e′VM algorithm was validated externally in an independent Swedish cohort, which suggests that this algorithm could be widely applicable in White populations.

ECHOCARDIOGRAPHIC PHENOTYPES. In the current study, LVEF and DD prevalence of the participants were similar to those of the general populations described in previous reports (45-48). Of note, in the present classification, both LVEDVi and LVMi were key components in classifying asymptomatic individuals into the proposed echocardiographic phenotypes. By contrast, GLS was not selected as a key marker for the e′VM algorithm despite its well-known performance to detect early alterations of LV systolic function in a range of populations (49,50). The echocardiographic phenotypes identified in the present analysis were notably similar to the phenotypic patterns of early cardiac alterations reported in diabetic patients (14). Indeed, using a cluster analysis based on echocardiographic parameters in 842 diabetic patients, Ernande et al. (14) highlighted 3 echocardiographic phenotypes including a "diastolic dysfunction" phenotype and "LVH with systolic dysfunction" phenotype. Despite the differing settings (general population vs diabetic patients), these findings would appear to reinforce our results and the possible ubiquitous nature of the echocardiographic phenotypes based on early and/or asymptomatic cardiac dysfunction. Furthermore, the prevalence of DD class 2016 assessment with conventional echo variables was very low in our cohort and remained similar in both D and D/S phenotypes, suggesting that the current definition of DD may be less relevant in an asymptomatic population.

The D phenotype was more frequent in women, whereas men were more likely to express diastolic changes with structural remodeling. The results reported by Ernande et al. were perceived as sex-specific echocardiographic patterns (14,51). However, our analysis showed similar patterns of echocardiographic phenotypes derived from men and women subgroups. The echocardiographic phenotypes proposed herein could thus provide robust identification of individuals regardless of sex difference.

Arterial stiffness is a fundamental contributor to increasing diastolic pressure (16,17) as well as impairing early systolic function (52). In the present study, (proximal to distal) vascular deteriorations were observed in both the D and the D/S phenotypes. Of note, PWV was similar in these 2 phenotypes. Underlying mechanisms following vascular abnormalities may potentially occur in these 2 phenotypes: the D phenotype may exhibit an early increase in intracardiac pressures in the absence of structural remodeling, while the D/S phenotype may further compensate the increase in afterload using increased LV volume and mass. This hypothesis could shed new

CENTRAL ILLUSTRATION **Echocardiographic Phenotypes in Asymptomatic Individuals**



Kobayashi, M. et al. J Am Coll Cardiol Img. 2021;■(■):■-■.

Among the 3 echocardiographic phenotypes, the e'VM echocardiographic-based algorithm (ie, mean e', left ventricular volume, and mass) differentially identified asymptomatic individuals with the "diastolic changes" phenotype and those with the "diastolic changes with structural remodeling" phenotype. The "diastolic changes" phenotype, consisting predominantly of women, displayed higher circulating levels of inflammatory biomarkers, whereas the "diastolic changes with structural remodeling" phenotype, consisted predominantly of men, displayed higher circulating levels of extracellular matrix remodeling biomarkers. Both echocardiographic phenotypes were associated with a higher risk of developing heart failure or cardiovascular death. CV = cardiovascular; HF = heart failure; IL1RL2 = Interleukin 1 Receptor Like 2; LVDVi = LVDV = left ventricule diastolic volume index; LVMi = left ventricular mass index; ST2 = soluble interleukin 2.

light on the early stage of the inter-relationship between cardiac and vascular parameters.

ECHOCARDIOGRAPHIC PHENOTYPES AND CIRCULATING BIOMARKERS ASSOCIATED WITH INFLAMMATION OR EXTRACELLULAR MATRIX REMODELING. Inflammation and extracellular matrix remodeling have been found to be associated with diastolic function (30,53). Paulus and Tschope (29) proposed a paradigm for HFpEF which highlighted the importance of a systemic proinflammatory state related to ageing, hypertension and obesity, further leading to the development of DD. In the current analysis, our results show that the D phenotype was significantly associated with increased levels of inflammatory biomarkers such as FABP4. Indeed, FABP4 is mainly expressed in adipose tissue and is an important mediator of inflammation, showing a significant link with DD (54,55) and a higher risk of cardiovascular events (56).

The D/S phenotype, on the other hand, was significantly associated with increased levels of CNP, ST-2, and troponin-I. CNP is an endothelial product released in response to sheer stress and has been associated with LV and LA remodeling in the general population (57). In addition, troponin-I and ST-2 may be prone to influencing the cumulative myocardial fibrotic process (58).

Our results, hence, support the fact that systemic inflammation may be associated with rising LV pressure with changes in diastolic function, whereas microvascular endothelial dysfunction and myocardial damage may be more closely related to cardiac structural remodeling, even in asymptomatic individuals.

CLINICAL IMPLICATIONS. In the latest American College of Cardiology/American Heart Association guidelines, an echocardiogram screening is recommended to identify those at high-risk of developing HF in individuals with hypertension (59) or slightly increased natriuretic peptide level (BNP: >50 pg/mL [Class IIa to IIb recommendation]) (60). Importantly, we show that the simple e′VM echocardiographic algorithm improved risk stratification on top of currently available scores such as the ARIC HF risk score and traditionally defined cardiac structure/function abnormalities (including DD class 2016 assessment), thus suggesting that additional echocardiogram-based screening could be encouraged. Of further importance, among the presented "high-risk" subgroups, DD class 2016 assessment with conventional echo variables only diagnosed <5% of individuals. Our results consequently suggest the importance of re-assessing echocardiographic data using the e′VM algorithm despite the absence of cardiac dysfunction according to conventional recommendations. We believe our echocardiographic phenotypes may serve as a new evidence-driven, integrated classification of individuals in preclinical settings with plausible circulating biomarkers and notable prognostic implications. How to manage individuals identified at high risk based on our algorithms is yet unknown. At least, given the higher risk of these individuals, a more careful follow-up could be undertaken. Whether the use of cardiovascular drugs could reduce the occurrence of HF in asymptomatic individuals requires testing. Importantly, the random forest model we built could be imbedded in health record systems to provide an automated identification of high-risk patients, maximizing the usefulness of echocardiogram in asymptomatic individuals.

STUDY LIMITATIONS. The main limitation of this study is its inherent observational design, based on a cross-sectional assessment; causality cannot therefore be inferred. The number of individuals with incident HF was relatively low, leading to moderate statistical power. The e′VM algorithm was derived from only echocardiographic variables; however, when adding additional clinical variables (ie, age, sex, comorbidities), the algorithm remained unchanged, suggesting that echocardiographic variables alone better predicted our phenotypes. In addition, the decision tree had numerically lower accuracy than the random forest, but this difference was moderate. This may be caused by some overoptimism in the decision tree accuracy statistics, as random forest are expected to perform sizably better than decision trees. As the cohort included relatively young individuals with a low comorbidity burden, the generalization of this phenotypes should be limited to individuals aged 50 to 70 years without overt cardiovascular disease. Further research is warranted to explore the applicability of our echocardiogram-based algorithm in older and sicker populations. In the STANISLAS cohort, individuals who had missing values for echocardiographic parameters used in cluster analysis were excluded. These latter individuals more often had cardiovascular risk factors. Echocardiographic data were acquired at different time periods in the STANISLAS and Malmö cohorts. However, the recommended measurement of echocardiographic parameters has not changed in the last 20 years (9–12). In the Malmö cohort, peak TR velocity was not quantified and was considered >2.8 cm/s as only a few individuals (<2%) have been reported to have a peak TR velocity greater than >2.8 cm/s in a similar population-based cohort (45). Importantly, in the Malmö cohort, LV end-diastolic volume and LA volume were not quantified; hence, these values were respectively estimated from LV diastolic diameter and LA surface area using a linear equation. This important limitation should trigger other external validations in prospective multicenter studies to improve the generalization of the e′VM algorithm. However, despite this limitation, the e′VM algorithm predicted outcomes in the Malmo cohort.

CONCLUSIONS

The present analysis allowed highlighting 3 echocardiographic phenotypes than can be easily identified in clinical practice using a simple algorithm (the e′VM algorithm). The 2 most abnormal phenotypes, namely "diastolic changes" and "diastolic changes with structural remodeling," exhibited significant differences in circulating biomarkers and the risk of HF and/or cardiovascular death. The authors believe that these echocardiographic phenotypes shed new light on our understanding of asymptomatic cardiac dysfunction, and our findings may have significant clinical implications in the design of HF prevention strategies. A further prospective multicenter study is

needed to assess the applicability of this e′VM algorithm.

ACKNOWLEDGMENTS The authors thank the Vandoeuvre-Lès Nancy Centre de Médecine Préventive staff and Dr Sophie Visvikis-Siest (Inserm U1122), who managed the STANISLAS Cohort for the first 3 visits. The authors also thank the staff of the Clinical Investigation Center and other personnel involved in the STANISLAS Cohort management: Biostatisticians R. Fay and Z. Lamiral, I.L. Machu; Computer scientists N. Boucenna, C. Gallina-Muller, P.L. Maclot, and T. Sas; Co-investigators K. Chau, P. Di Patrizio, D. Dobre, D. Gonthier, O. Huttin, L. Malingrey, V. Mauffrey, A. Olivier, T. Poyeton, E. Steyer, and G. Watfa; Data managers P. Cimon, E. Eby, and L. Merckle; Data entry operators M. Batsh, O. Blanger, C. Bottelin, N. Haskour, V. Jacquet, M.C. Przybylski, Y. Saribekyan, H. Thomas, and M. Vallee M; Echocardiographers M. Ben Sassi, S. Cario, Y. Camara, S. Coiro, Z. Frikha, A. Kearney-Schwartz, C. Selton-Suty, and G. Watfa; Imaging engineer: E. Bozec; Laboratory engineer J. Nuee-Capiaumont; Technicians J. Fruminet, M. Kuntz, J. Ravey, E. Rousseau, and C. Tachet; Project managers S. Bouali and C. Hertz; Quality engineer: X. Lepage; Registered nurses: M. Giansily, L. Poinsignon, N. Robin, M. Schmartz, M. Senn, E. Micor-Patrignani, and M. Toutlemonde; Hospital technician M.T. Fleurot; Resident physicians R. Alvarez-Vasquez, M. Amiot, M. Angotti, E. Babel, M. Balland, A. Bannay, P. Basselin, P. Benoit, J. Bercand, M. Bouazzi, E. Boubel, N. Boucherab-Brik N, F. Boyer, C. Champagne, S.A. Chenna, J. Clochey, D. Czolnowski, J. Dal-Pozzolo, L. Desse, B. Donetti, G. Dugelay, C. Friang, M. Galante, M. Garel, A. Gellenoncourt, A. Guillin, M.L. Hariton, M. Hinsiger, E. Haudiquet, J.M. Hubert, A. Hurtaud, J. Jabbour, S. Jeckel, A. Kecha, G. Kelche, C. Kieffert, E. Laurie're, M. Legay, A. Mansuy, O. Millet-Muresan, N. Meyer, E. Mourton, A.L. Naudé, A.C. Pikus, M. Poucher, M. Prot, A. Quartino, M. Saintot, A. Schiavi, R. Schumman, M. Serot, C. Sert, R. Siboescu, S. Terrier-de-la-Chaise, A. Thiesse, L. Thietry, M. Vanesson, and M. Viellard; Secretaries E. De Amorin E, C. Villemain, and N. Ziegler; Study coordinators E. Dauchy and S. Laurent; and all persons not listed above who helped in the funding, initiation, accrual, management, and analysis of the fourth visit of the STANISLAS cohort. And the authors thank the Nancy CHRU CRB Lorrain for its management of the biobank: the Steering committee: Pierre Mutzenhardt, Mehdy Siaghy, Patrick Lacolley, Marie-Ange Luc, Pierre-Yves Marie, and Jean-Michel Vignaud; the Advisory members Sophie Visvikis Siest and Faiez Zannad; the Technical committee, Christiane Branlant, Isabelle Behm-Ansmant, Jean-Michel Vignaud, Christophe Philippe, Jacques Magdalou, Faiez Zannad, and Patrick Rossignol; the Scientific committee: Laurence Tiret, Denis Wahl, Athanase Benetos, Javier Diez, Maurizio Ferrari, Jean-Louis Gueant, Georges Dedoussis, François Alla, François Gueyffier, Pierre-Yves Scarabin, Claire Bonithon Kopp, Xavier Jouven, Jean-Claude Voegel, and Jan Staessen. The Knut and Alice Wallenberg Foundation is also acknowledged for its generous support.

FUNDING SUPPORT AND AUTHOR DISCLOSURES

The STANISLAS Cohort visit 4 was sponsored by the Nancy CHRU and was funded in part by the Programme Hospitalier de Recherche Clinique Interrégional. Biomarker studies are co-funded by the French National Research Agency Fighting Heart Failure (ANR-15-RHU-0004) and FEDER Lorraine, and all French co-authors are supported by the French Programme d'investissements d'avenir project "Lorraine Université d'Excellence" GEENAGE (ANR-15-IDEX-04-LUE) programs, and the Contrat de Plan Etat Région Lorraine and FEDER IT2MP. The research leading to these results also received support from the European Union Commission's Seventh Framework program under grant 305507 (Heart OMics in Aging). Support was also provided from the "EXPERT" ERA-CVD 2016 and MR-Focus (both grants managed by the French National Research Agency). Drs. Girerd, Rossignol, and Zannad are supported by the French National Research Agency Fighting Heart Failure (ANR-15-RHU-0004), the French PIA project Lorraine Université d'Excellence GEENAGE (ANR-15-IDEX-04-LUE) programs, and the Contrat de Plan Etat Région Lorraine and FEDER IT2MP. Dr Girerd is a consultant for Novartis, AstraZeneca, and Boehringer Ingelheim. Dr Rossignol has received grants and personal fees from AstraZeneca, Bayer, CVRx, Fresenius, and Novartis; and personal fees from Grunenthal, Servier, Stealth Peptides, Vifor Fresenius Medical Care Renal Pharma, Idorsia, NovoNordisk, Ablative Solutions, G3P, Corvidia, and Relypsa. Dr Zannad has received personal fees from Boehringer Ingelheim, Janssen, Novartis, Boston Scientific, Amgen, CVRx, AstraZeneca, Vifor Fresenius, Cardior, Cereno Pharmaceutical, Applied Therapeutics, Merck Sharpe and Dohme, Bayer, and Cellprothera outside the submitted work; and has received other support from CVCT and Cardiorenal, outside the submitted work. Dr Ferreira is a consultant for Boehringer Ingelheim. Dr Magnusson is supported by grants from the Medical Faculty of Lund University; Skane University Hospital; the Crafoord Foundation; the Ernhold Lundstroms Research Foundation; the Region Skane; the Hulda and Conrad Mossfelt Foundation; the Southwest Skanes Diabetes Foundation; the Kockska Foundation; the Research Funds of Region Skåne; the Swedish Heart and Lung Foundation; and the Wallenberg Center for Molecular Medicine, Lund University. All other authors have reported that they have no relationships relevant to the contents of this paper to disclose.

ADDRESS FOR CORRESPONDENCE: Prof Nicolas Girerd, Centre d'Investigation Clinique Pierre Drouin-INSERM-CHRU de Nancy, Institut lorrain du coeur et des vaisseaux Louis Mathieu, 4, rue du Morvan, 54500 Vandoeuvre-Les-Nancy, France. E-mail: n.girerd@chru-nancy.fr.

PERSPECTIVES

COMPETENCY IN MEDICAL KNOWLEDGE: In asymptomatic individuals, a simple echocardiographic data-driven algorithm, based on e′, and LV volume and mass allows for identifying echocardiographic phenotypes with a high risk of developing HF.

TRANSLATIONAL OUTLOOK: Further research is needed to confirm the general applicability of the e′VM algorithm in the prevention of the development of overt HF in asymptomatic individuals.

REFERENCES

1. Yancy CW, Jessup M, Bozkurt B, et al. 2013 ACCF/AHA guideline for the management of heart failure: a report of the American College of Cardiology Foundation/American Heart Association Task Force on Practice Guidelines. *J Am Coll Cardiol*. 2013;62:e147–e239.

2. Kosmala W, Marwick TH. Asymptomatic left ventricular diastolic dysfunction predicting progression to symptomatic heart failure. *J Am Coll Cardiol Img*. 2020;13:215–227.

3. Ammar KA, Jacobsen SJ, Mahoney DW, et al. Prevalence and prognostic significance of heart failure Stages: application of the American College of Cardiology/American Heart Association heart failure staging criteria in the community. *Circulation*. 2007;115:1563–1570.

4. Cohn JN, Ferrari R, Sharpe N. Cardiac remodeling–concepts and clinical implications: a consensus paper from an international forum on cardiac remodeling. On behalf of an International Forum on Cardiac Remodeling. *J Am Coll Cardiol*. 2000;35:569–582.

5. Pfeffer MA, Braunwald E. Ventricular remodeling after myocardial infarction. Experimental observations and clinical implications. *Circulation*. 1990;81:1161–1172.

6. Tokodi M, Shrestha S, Bianco C, et al. Interpatient similarities in cardiac function; a platform for personalized cardiovascular medicine. *J Am Coll Cardiol Img*. 2020;13:1119–1132.

7. Mogelvang R, Sogaard P, Pedersen SA, Olsen NT, Schnohr P, Jensen JS. Tissue Doppler echocardiography in persons with hypertension, diabetes, or ischaemic heart disease: the Copenhagen City Heart Study. *Eur Heart J*. 2009;30:731–739.

8. Dalen H, Thorstensen A, Romundstad PR, Aase SA, Stoylen A, Vatten LJ. Cardiovascular risk factors and systolic and diastolic cardiac function: a tissue Doppler and speckle tracking echocardiographic study. *J Am Soc Echocardiogr*. 2011;24:322–332.

9. Nagueh SF, Smiseth OA, Appleton CP, et al. Recommendations for the evaluation of left ventricular diastolic function by echocardiography: an update from the American Society of Echocardiography and the European Association of Cardiovascular Imaging. *J Am Soc Echocardiogr*. 2016;29:277–314.

10. Nagueh SF, Appleton CP, Gillebert TC, et al. Recommendations for the evaluation of left ventricular diastolic function by echocardiography. *Eur J Echocardiogr*. 2009;10:165–193.

11. Paulus WJ, Tschope C, Sanderson JE, et al. How to diagnose diastolic heart failure: a consensus statement on the diagnosis of heart failure with normal left ventricular ejection fraction by the Heart Failure and Echocardiography Associations of the European Society of Cardiology. *Eur Heart J*. 2007;28:2539–2550.

12. Appleton CP. Doppler assessment of left ventricular diastolic function: the refinements continue. *J Am Coll Cardiol*. 1993;21:1697–1700.

13. Huttin O, Fraser AG, Coiro S, et al. Impact of changes in consensus diagnostic recommendations on the echocardiographic prevalence of diastolic dysfunction. *J Am Coll Cardiol*. 2017;69:3119–3121.

14. Ernande L, Audureau E, Jellis CL, et al. Clinical implications of echocardiographic phenotypes of patients with diabetes mellitus. *J Am Coll Cardiol*. 2017;70:1704–1716.

15. Shah SJ, Katz DH, Selvaraj S, et al. Phenomapping for novel classification of heart failure with preserved ejection fraction. *Circulation*. 2015;131:269–279.

16. Kang S, Fan HM, Li J, et al. Relationship of arterial stiffness and early mild diastolic heart failure in general middle and aged population. *Eur Heart J*. 2010;31:2799–2807.

17. Cauwenberghs N, Knez J, D'Hooge J, et al. Longitudinal changes in LV structure and diastolic function in relation to arterial properties in general population. *J Am Coll Cardiol Img*. 2017;10:1307–1316.

18. Ferreira JP, Girerd N, Bozec E, et al. Cohort profile: rationale and design of the fourth visit of the STANISLAS cohort: a familial longitudinal population-based cohort from the Nancy region of France. *Int J Epidemiol*. 2018;47:395–495.

19. Berglund G, Nilsson P, Eriksson KF, et al. Long-term outcome of the Malmo preventive project: mortality and cardiovascular morbidity. *J Intern Med*. 2000;247:19–29.

20. Ferreira JP, Girerd N, Bozec E, et al. Intima-media thickness is linearly and continuously associated with systolic blood pressure in a population-based cohort (STANISLAS cohort study). *J Am Heart Assoc*. 2016;5:e003529.

21. Lang RM, Badano LP, Mor-Avi V, et al. Recommendations for cardiac chamber quantification by echocardiography in adults: an update from the American Society of Echocardiography and the European Association of Cardiovascular Imaging. *J Am Soc Echocardiogr*. 2015;28:1–39.

22. Tsugu T, Postolache A, Dulgheru R, et al. Echocardiographic reference ranges for normal left ventricular layer-specific strain: results from the EACVI NORRE study. *Eur Heart J Cardiovasc Imaging*. 2020;21:896–905.

23. Coiro S, Huttin O, Bozec E, et al. Reproducibility of echocardiographic assessment of 2D-derived longitudinal strain parameters in a population-based study (the STANISLAS Cohort study). *Int J Cardiovasc Imaging*. 2017;33:1361–1369.

24. Frikha Z, Girerd N, Huttin O, et al. Reproducibility in echocardiographic assessment of diastolic function in a population based study (the STANISLAS Cohort study). *PLoS One*. 2015;10:e0122336.

25. Van Bortel LM, Laurent S, Boutouyrie P, et al. Expert consensus document on the measurement of aortic stiffness in daily practice using carotid-femoral pulse wave velocity. *J Hypertens*. 2012;30:445–448.

26. Laurent S, Cockcroft J, Van Bortel L, et al. Expert consensus document on arterial stiffness: methodological issues and clinical applications. *Eur Heart J*. 2006;27:2588–2605.

27. Goncalves N, Gomes-Ferreira C, Moura C, et al. Worse cardiac remodeling in response to pressure overload in type 2 diabetes mellitus. *Int J Cardiol*. 2016;217:195–204.

28. Sabbah MS, Fayyaz AU, Denus Sd, et al. Obese-inflammatory phenotypes in heart failure with preserved ejection fraction. circulation. *Circ Heart Fail*. 2020;13:e006414.

29. Paulus WJ, Tschope C. A novel paradigm for heart failure with preserved ejection fraction: comorbidities drive myocardial dysfunction and remodeling through coronary microvascular endothelial inflammation. *J Am Coll Cardiol*. 2013;62:263–271.

30. Tromp J, Khan MA, Klip IT, et al. Biomarker profiles in heart failure patients with preserved and reduced ejection fraction. *J Am Heart Assoc*. 2017;6:e003989.

31. Tromp J, Westenbrink BD, Ouwerkerk W, et al. Identifying pathophysiological mechanisms in heart failure with reduced versus preserved ejection Fraction. *J Am Coll Cardiol*. 2018;72:1081–1090.

32. Collier P, Watson CJ, Voon V, et al. Can emerging biomarkers of myocardial remodeling identify asymptomatic hypertensive patients at risk for diastolic dysfunction and diastolic heart failure? *Eur J Heart Fail*. 2011;13:1087–1095.

33. Hage C, Michaelsson E, Linde C, et al. Inflammatory biomarkers predict heart failure severity and prognosis in patients with heart failure with preserved ejection fraction: a holistic proteomic approach. *Circ Cardiovasc Genet*. 2017;10:e001633.

34. Sanders-van Wijk S, van Empel V, Davarzani N, et al. Circulating biomarkers of distinct pathophysiological pathways in heart failure with preserved vs. reduced left ventricular ejection fraction. *Eur J Heart Fail*. 2015;17:1006–1014.

35. Enroth S, Maturi V, Berggrund M, et al. Systemic and specific effects of antihypertensive and lipid-lowering medication on plasma protein biomarkers for cardiovascular diseases. *Sci Rep*. 2018;8:5531.

36. Leosdottir M, Willenheimer R, Plehn J, et al. Myocardial structure and function by echocardiography in relation to glucometabolic status in elderly subjects from 2 population-based cohorts: a cross-sectional study. *Am Heart J*. 2010;159:414–420.

37. Khouri SJ, Maly GT, Suh DD, Walsh TE. A practical approach to the echocardiographic evaluation of diastolic function. *J Am Soc Echocardiogr*. 2004;17:290–297.

38. Lang RM, Bierig M, Devereux RB, et al. Recommendations for chamber quantification: a report from the American Society of Echocardiography's Guidelines and Standards Committee and the Chamber Quantification Writing Group, developed in conjunction with the European Association of Echocardiography, a branch of the European Society of Cardiology. *J Am Soc Echocardiogr*. 2005;18:1440–1463.

39. Sengupta PP, Shrestha S, Berthon B, et al. Proposed requirements for cardiovascular imaging-related machine learning evaluation (PRIME): a checklist: reviewed by the American College of Cardiology Healthcare Innovation Council. *J Am Coll Cardiol Img*. 2020;13:2017–2035.

40. Therneau T, Atkinson B. B. R. rpart: Recursive partitioning and regression trees. R package version 4.1-11. Available at: https://CRAN.R-project.org/package = rpart. Accessed May 1, 2018.

41. Liaw A, Wiener M. *Classification and regression by random forest*. 2007.

42. Kuhn M. Building predictive models in R using the caret package. *J Stat Softw*. 2008;028.

43. Jacobs L, Efremov L, Ferreira JP, et al. Risk for incident heart failure: a subject-Level Meta-analysis from the heart "OMics" in AGEing (HOMAGE) Study. *J Am Heart Assoc*. 2017;6:e005231.

44. Agarwal SK, Chambless LE, Ballantyne CM, et al. Prediction of incident heart failure in general practice: the Atherosclerosis Risk in Communities (ARIC) Study. *Circ Heart Fail*. 2012;5:422–429.

45. Almeida JG, Fontes-Carvalho R, Sampaio F, et al. Impact of the 2016 ASE/EACVI recommendations on the prevalence of diastolic dysfunction in the general population. *Eur Heart J Cardiovasc Imaging*. 2018;19:380–386.

46. Kane GC, Karon BL, Mahoney DW, et al. Progression of left ventricular diastolic dysfunction and risk of heart failure. *JAMA*. 2011;306:856–863.

47. Yeboah J, Rodriguez CJ, Stacey B, et al. Prognosis of individuals with asymptomatic left ventricular systolic dysfunction in the multi-ethnic study of atherosclerosis (MESA). *Circulation*. 2012;126:2713–2719.

48. Wang TJ, Evans JC, Benjamin EJ, Levy D, LeRoy EC, Vasan RS. Natural history of asymptomatic left ventricular systolic dysfunction in the community. *Circulation*. 2003;108:977–982.

49. Huttin O, Girerd N, Coiro S, et al. Association between layer-specific longitudinal strain and risk factors of heart failure and dyspnea: a population-based study. *J Am Soc Echocardiogr*. 2019;32:854–865.

50. Potter E, Marwick TH. Assessment of left ventricular function by echocardiography: the case for routinely adding global longitudinal strain to ejection fraction. *J Am Coll Cardiol Img*. 2018;11:260–274.

51. Kannel WB, McGee DL. Diabetes and cardiovascular disease. The Framingham study. *JAMA*. 1979;241:2035–2038.

52. Borlaug BA, Melenovsky V, Redfield MM, et al. Impact of arterial load and loading sequence on left ventricular tissue velocities in humans. *J Am Coll Cardiol*. 2007;50:1570–1577.

53. Zile MR, Jhund PS, Baicu CF, et al. Plasma biomarkers reflecting profibrotic processes in heart failure with a preserved ejection fraction: data from the prospective comparison of ARNI with ARB on management of heart failure with preserved ejection fraction study. *Circulation Heart Fail*. 2016;9.

54. Baessler A, Lamounier-Zepter V, Fenk S, et al. Adipocyte fatty acid-binding protein levels are associated with left ventricular diastolic dysfunction in morbidly obese subjects. *Nutr Diabet*. 2014;4:e106.

55. Chan MM, Santhanakrishnan R, Chong JP, et al. Growth differentiation factor 15 in heart failure with preserved vs. reduced ejection fraction. *Eur J Heart Fail*. 2016;18:81–88.

56. Floresta G, Pistarà V, Amata E, et al. Adipocyte fatty acid binding protein 4 (FABP4) inhibitors. A comprehensive systematic review. *Eur J Med Chem*. 2017;138:854–873.

57. Sangaralingham SJ, McKie PM, Ichiki T, et al. Circulating C-type natriuretic peptide and its relationship to cardiovascular disease in the general population. *Hypertension*. 2015;65:1187–1194.

58. Bayes-Genis A, de Antonio M, Vila J, et al. Head-to-head comparison of 2 myocardial fibrosis biomarkers for long-term heart failure risk stratification: ST2 versus galectin-3. *J Am Coll Cardiol*. 2014;63:158–166.

59. Whelton PK, Carey RM, Aronow WS, et al. 2017 ACC/AHA/AAPA/ABC/ACPM/AGS/APhA/ASH/ASPC/NMA/PCNA guideline for the prevention, detection, evaluation, and management of high blood pressure in adults: a report of the American College of Cardiology/American Heart Association Task Force on Clinical Practice Guidelines. *J Am Coll Cardiol*. 2018;71(19):e127–e248.

60. Yancy CW, Jessup M, Bozkurt B, et al. 2017 ACC/AHA/HFSA focused update of the 2013 ACCF/AHA guideline for the management of heart failure: a report of the American College of Cardiology/American Heart Association Task Force on Clinical Practice Guidelines and the Heart Failure Society of America. *J Am Coll Cardiol*. 2017;70:776–803.

KEY WORDS biomarkers, cardiovascular diseases, cluster analysis, echocardiogram, heart failure, machine learning, prognosis

APPENDIX For supplemental figures and tables, please see the online version of this paper.